University of Bath

Design, fabrication, and validation of passive wireless resonant sensors for NDT/SHM

O. Iervolino and Michele Meo

Material Research Centre, Department of Mechanical Engineering, University of Bath, Bath, BA2

7AY, UK

Abstract

Detection of visible crack, delamination etc. in composite structures can be fulfilled by several techniques. However, the problem is of greater complexity in the case of nonvisible defects such as barely visible impact damage and microcracks.

The objective of this research work was to create and validate a low cost smart-sensor for NDT and structural health monitoring (SHM) to be used for complex geometries. The smart-sensor presents a dual function, i.e. it determines the presence of delamination and cracks within the cross-section but it also provides information on surface damages due to fatigue or impacts. In the latter case the damage could induce the breakage of the sensor that could still work with a different resonant frequency.

The sensor utilizes a passive wireless resonant telemetry scheme based on an inductor capacitor (LC). The use of a passive system eliminates the need for onboard power and exposed interconnects, increasing the life of the device and the reliability due to the continuous operation even in case of damage results from the sensor.

The sensor design, the signal processing and the experimental setup that validate the remote interrogation of the antenna sensor are presented. Two different designs were investigated, one for conductive surface and one for nonconductive surface (fiberglass-composite).

1. Introduction

Structural Health Monitoring (SHM) aims to provide information on the current state of structures giving a diagnosis of the "state" of the structure. Structural Health Monitoring can be considered as a new and improved way to make an in-situ Non-Destructive Evaluation, where data transmission, computational power, integration of sensor, use of smart material etc… are involved. Given the complexity and weight penalties associated with the installation of wired sensors [2, 3], wireless sensors are a promising solution to overcome these issues. Furthermore, with the steady increase of the use of composite materials in the aerospace industry, much attention has been devoted to smart material and structures with embedded sensors to provide an early warning signs of damage occurrence, resulting into potentially more efficient systems and safer structures [4-9].

Standard transducers requires for its operations an electrical current, usually generated by a power supply. Typically a sensor needs to detect a specified change and transfer the information to the data acquisition system. Wired transducers due the necessity of connects by wires for power and data transmission became more complex to install and maintain, becoming typically a cost increase. As a consequence, a number of studies are being conducted to design and manufacture passive wireless

sensors [9, 10] despite the fact that wired sensors remain one of the most practical solutions for in-situ measurements.

A resonant sensor, with the ability to work wireless and wired (using the same principles), is presented in this work. Two working concept are presented: 1) wireless data transmission without the necessity of battery, being interrogated by an external antenna, 2) connecting a wire directly on the sensor. The sensor's thickness is less than 1 millimetre and it was printed on a flexible substrate allowing the possibility to be easily embedded inside a laminated structures or bonded on complex structures. The wired sensors could work as a SHM sensor, offering the possibility to monitor structures in real time. While the wireless systems, using an external loop probe, is more suitable for ground inspection, acting as an NDE sensor. Another great advantage of the sensor presented in this work is the ability to monitor both conductive and non-conductive structure, one of the main challenges commonly encountered for resonant circuit [11, 12]. The resonant sensor [13] acting as an inductor with a single conductive trace, if damaged, could continue to work. The main difference will be the change of its own resonant frequency due to the reduced length of the path of the sensor, hence the sensor presents fissiparous properties. Two sensors were present on this work, investigating two different techniques for the manufacturing of the sensor. The first sensor present a thickness of 110um, realized with an etching process on a flexible polyimide sheet, using copper as a conductive trace. The second sensor, having a thickness of 2mm, was realized using a Printed Circuit Board (PCB) with FR4 as substrate and copper on the surface. The conductive trace was realized using a milling machine. The first sensor, due is thickness and the flexibility and the resistivity of the polyimide, could be easily embedded inside a structure or surface mounted, adapting easily to curved shapes while the second sensor offers a low-cost manufacturing solution.

2. Sensor's principle of function

Composite structures can exhibit barely visible damage (BVID) not visible on the external surface, but can cause a loss in structural integrity; presenting a challenge in the detection of delamination or crack within the composite panel. The sensor presented has the great potentiality to be sensible also to this kind defect. CFRP (Carbon Fiber Reinforce Polymer) panel with delaminate were tested and detected with the sensor presented. The main idea was to transform a defect strain, crack, BVID, or a changing of the material properties into the change in the resonant frequency, bandwidth, peak distribution, amplitude of the signal generated by the sensor. In this work, the resonant frequency represents the principal parameter of investigation. Indeed starting from the governing equation of resonant frequency it is possible to highlight the parameters responsible for the shift of the resonant frequency when a change in the structure or in the material properties occurs.

$$f = \frac{1}{2\pi\sqrt{LC}}$$
(1)

The variable parameters influencing the resonant frequency are the inductance L and the capacitance C. First of all it is important to highlight how the resonant frequency is related to the shape of the circuit, the permeability of the material used for the support and the coated material (in our case the air). The sensor used is a square spirals resonant circuit, characterized by a single conductive trace (copper) on a dielectric substrate (polyimide or FR4), with the turn's spiral all the way to the centre of the coil as reported in the Figure 1. The sensor design was based on the SansEC sensor [14], having a conductive trace with a width (*w*) of 2mm and a gap (*g*) of 0.13 mm between neighbouring traces, and an overall squared area of 10cm^2 of side (*l*).
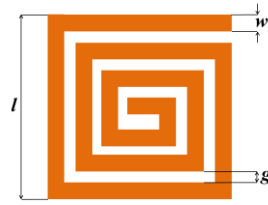
a)   Geometry design

Figure 1- Example of geometry of the spiral sensor

The resonant sensor acts as an electrical inductor in the form of a planar spiral. It consists of an inductor element, a capacitor element, and a resistor element. As mentioned before, two different manufacturing processes were investigated, realizing, as illustrated in Figure 2, two sensors with the same parameters' design (*g,w,l*). The sensors on the polyimide substrate, due their slenderness and the easiness to bend themselves are fixed on a polyethylene layer 1mm thin and then located on the sample to test. Furthermore the use of a polyethylene layer ensures a uniform gap between the sensor and the material to be tested during the comparison between the reference test and the sample damaged, offering a more accurate repeatability of the measurements.
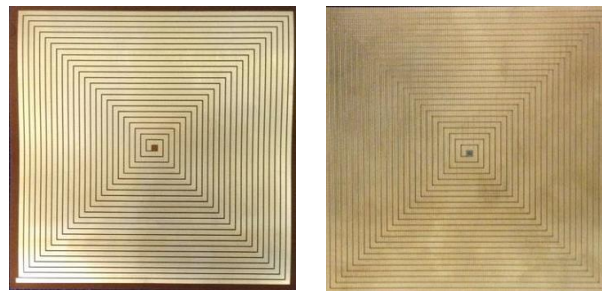
a)   Copper trace on   b)   Copper trace on
     polyimide layer   FR4 substrate

Figure 2 Spiral Resonant Sensors realized with different techniques

The understanding of the sensing function and the performance of the sensor are based on the estimation of the parameters of the sensors based on the equivalent electrical circuits. Indeed, the sensor is represented by the lumped model of an LC tuned circuit, as showed in Figure 3a. Since the sensor itself is an inductor, the inevitable resistance and capacitance are considered parasitic, although in our case present relevant parameters to be examined to detect the physical properties for which the sensors measure. The inductance is represented by the sensor itself, in particular to the conductive trace wounded to constitute a helix, and is mainly related to the number of turns per given area. The Capacitance is a result of the distance between the conductive trace and the sequence and properties of the underlying layers. The LC circuit, is a theoretical model, taking in account the real circuit, a resistance has to be take in account, in particular the one related to the inductance. In Figure 3b a series resistance is added to the inductance to take in account the opposition to the current given by the conductive trace itself, related to his length his geometries (ex. Round corner could reduce the resistance).
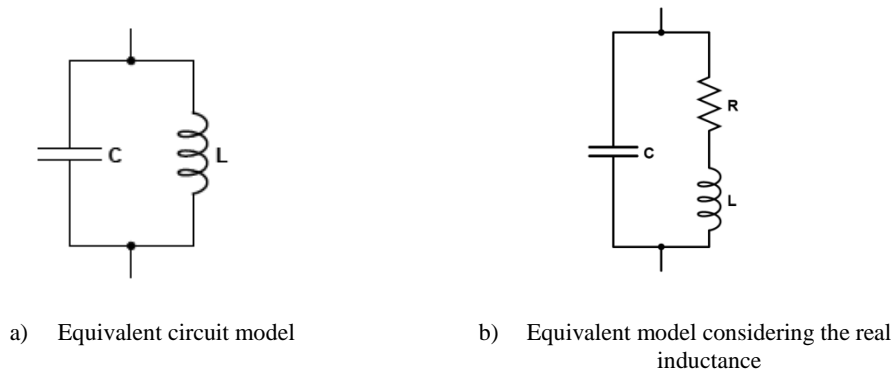
a) Equivalent circuit model

b) Equivalent model considering the real inductance

Figure 3 equivalent circuit model of the sensor, a) ideal LC tuned circuit, b) considering a real inductance

Resistance, Inductance and capacitance represent the sensor key parameters, and they will now be treated one by one. The sensors acting as a tuned circuit could be designed to change correspondingly to the physical state for which the sensor is measuring, as pressure, temperature, PH (14-17) and all physical characteristics affecting the parameter of the RLC circuit.

2.1. Inductance

The inductance is the ratio of total magnetic flux (the magnetic flux multiplied the number of turns N) to current through the inductor.

$$L = \frac{N\phi}{I} \qquad (2)$$

The total inductance of the coil is equal to the sum of the self-inductance of each straight segment plus the mutual inductance of the trace interaction. The mutual inductance is related to the mutually coupled magnetic fields of adjacent traces, and depends on the distance of the trace, the direction of the current and the geometries of the conductive trace). In fact the term regarding the mutual inductance is split in two parts, due to the dependence of the mutual inductance with the directions of current on conductors, being positive M_+ when the current flow in the same direction and negative M_- when they are in the opposite directions; while the Self-inductance is the ratio between the current carrying conductor and the current passing through it.

$$L = L_s - (M_+ + M_-) \qquad (3)$$

As highlighted by Neagu (18), using the formula (4), of the self-inductance of a rectangle having diameter l, thickness w and height h (Figure 4); the self-inductance increase with decreasing the height of the trace:
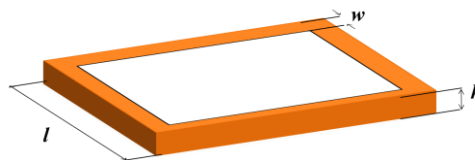

Figure 4 Rectangle with diameter l, thickness w and height h

$$L_{s(N=1)} = \frac{2\mu l}{\pi}\left[\ln\frac{4l}{w+h} + 0.894\frac{w+h}{4l} - 0.660\right] \tag{5}$$

It is reasonable to assume, that the formula keep the same correlation with the increasing number of turns. On the contrary, the thickness b has its own correlation with the number of turns, considering that the number of possible spiral on the same area is strictly related to the width of the trace and they are related to other parameters, as reported in this work. This consideration on the self-inductance brings to the optimization of the inductance increasing the perimeter of the conductive trace keeping the total covered area constant. These leads to the choice of adopt a square spiral rather than a circular one.

2.2. Resistance

The physical parameter influencing the resistance of the sensors are the resistance of the conductive trace, equal to a series of resistances, and the resistance of the underlying layer, accounting as parallel resistance. The series resistance, consist of two terms that differs from each other, function of their dependence with the frequency. The frequency-independent term is the DC resistance of the wire of length l, thickens h, with b and made of a material of resistance ρ, expressed through the Ohm's law in the formula below.

$$R_s = \frac{\rho l}{hb} \tag{6}$$

The frequency-dependent contribution of the series resistance, are related to the eddy current and to the skin depth, strictly interconnected between each other. The eddy-currents are local current travelling with opposite direction respect to the applied current, arising from a changing of magnetic field. The eddy current will reinforce the current on the skin of the conductive trace resulting in cancelling the current in the middle. This phenomenon takes is usually called skin-depth, denoted as δ_{trace}. According to the equation below, the skin-depth is related to the properties of the material and to the frequency of the current. In particular increasing the frequency the current distribution change, and tend to concentrate on the edge of the wire. This parameter became relevant when its value is less than the dimension of the conductive trace.

$$\delta_{trace} = \sqrt{\frac{2\rho}{\omega\mu}} \tag{7}$$

Regarding our sensor, considering the copper as conductive trace and a frequency range of about 25-35MHz, the skin depth is $\delta_{trace} \approx 30\mu m$. Moreover, the magnetic field causes eddy current also on the adjacent trace and in the underlying conductive substrate (in our case the carbon composite). Regarding the eddy current on the underlying layer, the magnetic field, can penetrate as seen before, only a limited distance, which as before could be evaluated through the penetration depth. As reported by (11) using the parameter of the carbon composite for aerospace application and considering the same order of magnitude for the frequency the penetration depth is $\delta_{ulayer} \approx 1mm$. Regarding the parallel resistance is related to the insulating layer underneath the sensor, and is far less than that of the series resistance. For the purpose of this paper we refer for the formula of the parallel resistance to (18).

2.3. Capacitance

The Capacitance is strictly related to the type of sequence of underlying layer. The sensors are surface mounted along the samples so all test execute in this work could be related to three kinds of different setups with different consequence on the parasitic capacitance. For simplicity, we focused only on the effect of two adjacent conductive traces, considering non relevant the effect of the other traces and the edge effects. The sensor's substrates (FR4 and polyimide) act both as dielectric, having the same behaviour in the reported configurations.
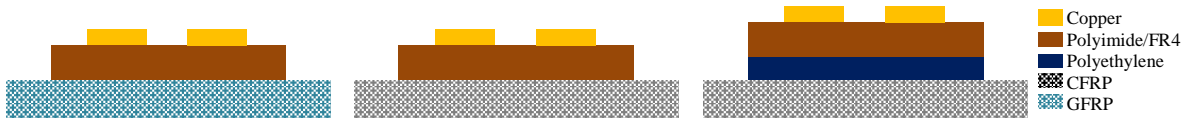

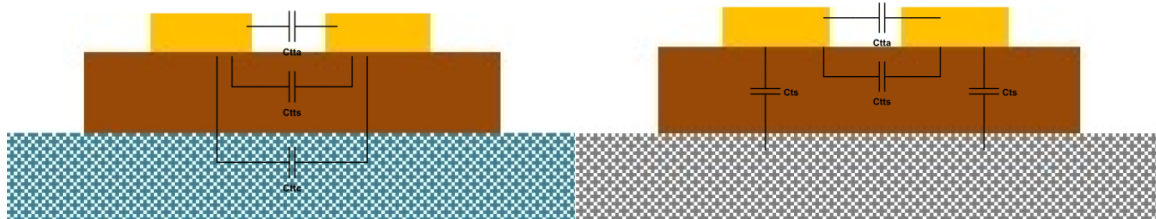**Figure 5 Cross section of spiral sensor on different substrate**

Figure 6 Cross section showing the parasitic capacitance

In the first configuration, formed by the sensor placed on the GFRP (Glass Fiber Reinforce Polymer), the parasitic capacitance is the results of two contributions affected by three insulating layers. The first parameter is the capacitance between adjacent turns C_{tta} considering the air gap as dielectric. Instead the second parameter is the capacitance between the coil's turn C_{tts} considering the underlying layer as dielectric. If the substrate on which the coil is positioned is relatively thin, it has to be taking in account in the second parameter another capacitance C_{ttc} added in parallel. The latter parameter is relevant for the detection of the material's integrity, as reported by (19, 20).

In the second configuration, formed by the sensor placed on the CFRP, due the conductivity of the material, the parameter contributing the parasitic capacitance are three: the first C_{tta} and the second terms C_{tts} are the same of the previous model, with the only difference that the carbon composite does not contribute as capacitance, and so the term C_{tts} is due only to the isolating layer under the sensor. The third parameter that contributes to the parasitic capacitance is the C_{ts}, the capacitance between the conductive trace and the substrate. If the material, as in the case of carbon composite, present a notable conductivity, the term C_{ts} became the most relevant contribution to the parasitic capacitance, in particular, as for our sensor design the height of the conductive trace are much smaller than the coil area, the term C_{tta} became negligible. The formula for the evaluation of all defined parameters, and their dependence to the characteristic of the sensor and the material used are reported by Neagu and Jow (18, 21).

The third configuration, having the polyethylene layer under the FR4, behaves as the second, with the only difference of presenting, another capacitance C_{tp} added in series to C_{ts}, and another capacitance C_{ttp} in parallel to C_{tts}.

3. Experimental setup

3.1. Interrogation method

Based on the capacity of the resonant structures to act as antenna when excited, and then exacerbating radiated emission, it is possible to determine the self-resonance frequency [22], by using a spectrum analyser with an internal tracking generator, a loop antenna and a directional coupler. More precisely a swept input frequency was send by the tracking generator to the loop probe. The loop antenna connected through the directional coupler, reflects most of the incident energy it receives, which is send directly in to the spectrum analyser. This configuration can act as an absorption wave meter. Indeed when a structure, with a natural resonant frequency within the swept-frequency range, is in the proximity of the probe its resonant frequency can be visualized as a dip in the spectrum trace. The presence of the change is caused by an incident RF absorbed by the structure. So when the resonant frequency is known, a short swept range has to be refined in order to increase the sensitivity of the sensor and allowing determining a change in the structure due to the presence of a defect. Indeed the comparison of resonant frequency of the same/similar samples before and after a damage occurs offers the possibility to detect its presence.

This effect is subtle and can easily be missed or misunderstood, so great accuracy is required, in order to compare the resonant frequency. It must be noted that a change in the instrumentation, surrounding environments could affect the measure leading to false alarm. Furthermore, regarding the distance between the loop antenna and the passive sensors, it is recommend to set the distance at 1/10 of the wavelength. Indeed a current flowing into the coil (loop antenna) radiates a near-magnetic field that falls off with r^{-3}. Regarding the interrogation system, and the final destination of the sensor, designed to work mainly in aerospace sector, in order to avoid electromagnetic interference with the frequency adopted in the aeronautics, the sensors' frequencies should be less than 74.8 MHz (marker beacon) or greater than 1220 MHz (Distance Measuring Equipment (DME)).

3.2. Test plan

Two different samples were tested, a GFRP (non-conductive sample), and a CFRP (conductive sample). The spiral sensor was activated adopting either a wireless and wired setup. In the first method, Figure 7, the magnetic field is induced in the sensor through a loop antenna connected, through a coupler, to the generator output of the spectrum analyser. The sensor, due its design geometries, could be considered as a resonant structure acting as an antenna, exacerbating radiated emissions.
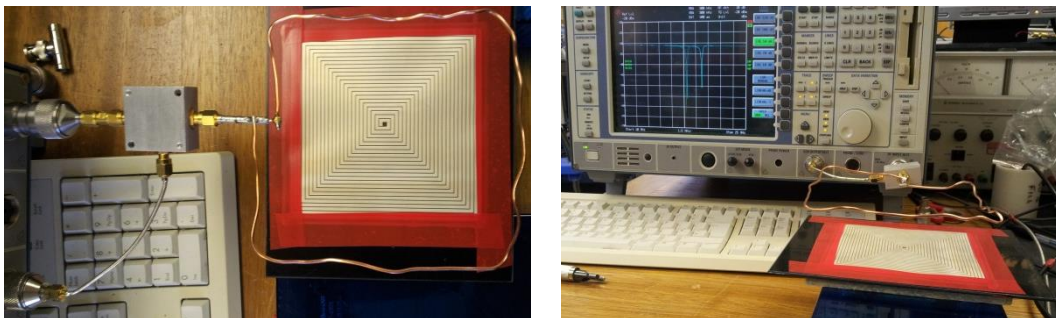
Figure 7 Wireless setup: a) Top-view, b) Front-view

In the second method, Figure 8, the sensor is wired directly to both ends of the conductive trace and then connected directly to the output generator. The wired setup was chosen to better understand the sensitive parameters affecting its performance, reducing the parameters affecting the functioning of performance such as the mutual inductance between the loop and the sensor. Furthermore, the wired setup reduces the shielding of signal when conductive samples (CFRP) are tested. The wireless system was tested only with non-conductive samples, in order to avoid shielding effect and to proof the potentiality of the spiral sensor to work wireless.
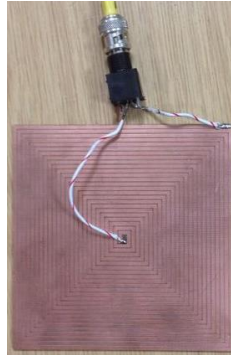

Figure 8 Wired setup

In order to determine the presence of damage inside the samples, and to ensure the repeatability of the experiments, the following experimental procedure was followed. Different samples were manufactured using the autoclave in a single shot to ensure the consistency of the manufacturing method. All samples were tested with the wireless and the wired approach, using the spiral sensor. After ensuring that all samples of the same type, had the same resonant frequency, different damage were performed on the samples, leaving one sample intact as reference, in order to compare the resonant frequency and verify the detection of damage. As reported in Table 1, two types of damage were investigated; holes obtained using a driller, and two impacts, at different energies, causing a barely visible impact damage and a visible crack on the opposite face to the impact (barely visible in the front impacted face), as illustrated in the Figure 10. The specifications of the samples used and the characteristics of the damage are reported in the table below.

Table 1 Samples and defects characteristics

Material	Samples Thickness	Lamination sequence	Hole		Impact	
			Hole1	Hole2	BVID 1	BVID 2
CFRP	1.30mm	$[(\pm45)_2/F/(\bar{F})]_S$	2mm Φ	5mm Φ	Impact 10 J	Impact 12 J
GFRP	5.80mm	$[0/90]_{5S}$	9mm Φ			

a)   CFRP Intact   b)   CFRP Hole 1   c)   CFRP Hole 2   d)   CFRP Impact 10J   e)   CFRP Impact 12J
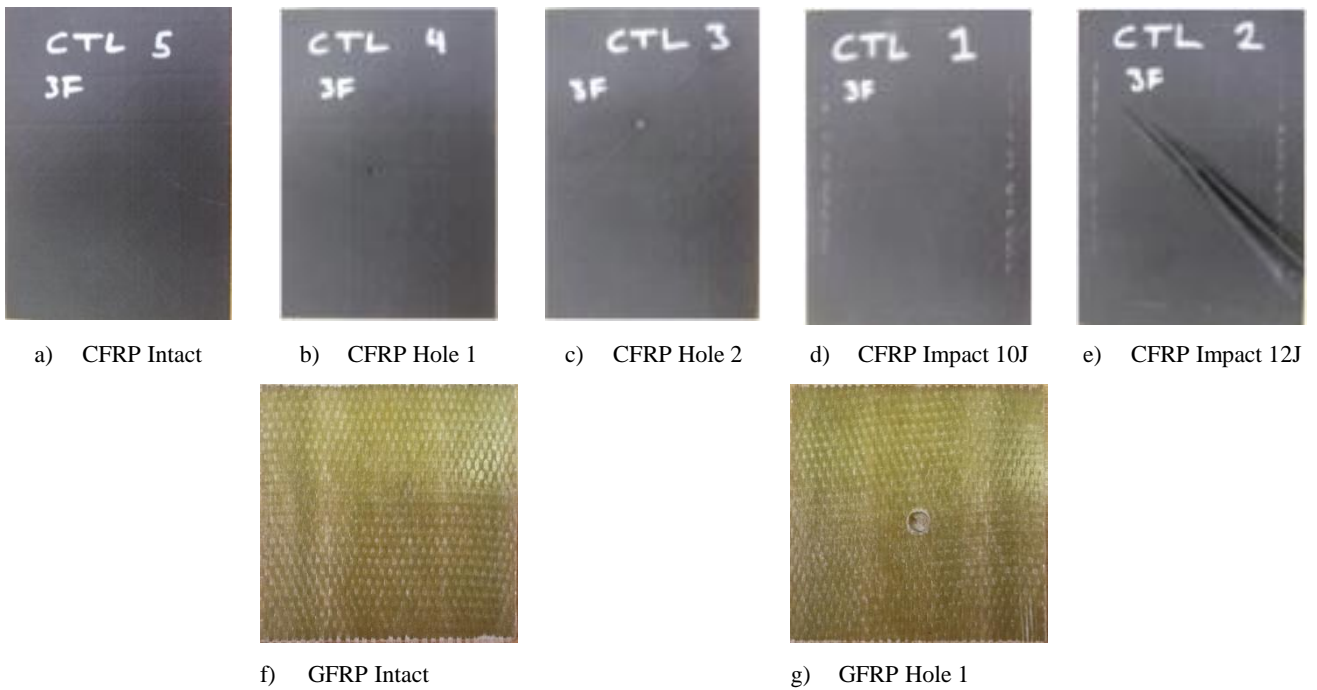
f)   GFRP Intact   g)   GFRP Hole 1

Figure 9 Composites panel tested

The impacted samples were also investigated using the infrared thermography to have a comparative NDT technique (Figure 10a) especially for the sample impacted with a low energy (10J).

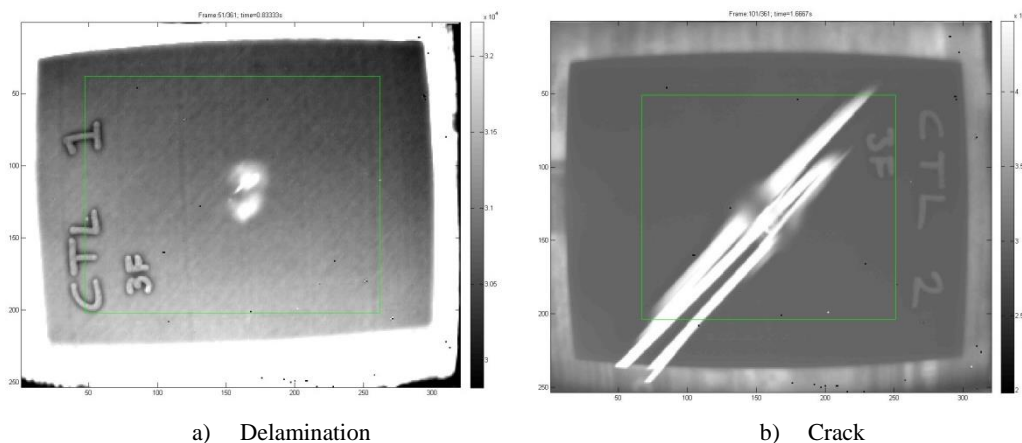
a)   Delamination   b)   Crack

Figure 10 Thermography test: a) CFRP sample impacted with 10 J, showing a delamination in the middle; b) CFRP sample impacted with 12J showing a visible crack

3.3. Wireless setup:

As described before, the loop antenna is attached to the spectrum analyser through a coupler and the sensor (etched on polyimide) is placed on the sample under test. Two interrogation distances were investigated: 50 and 90 mm respectively. Due the high sensibility of the sensor, in order to minimize the interference with the surrounding environment the sample were positioned by minimizing the contact with other objects, using media that will support the sample only on the edges.
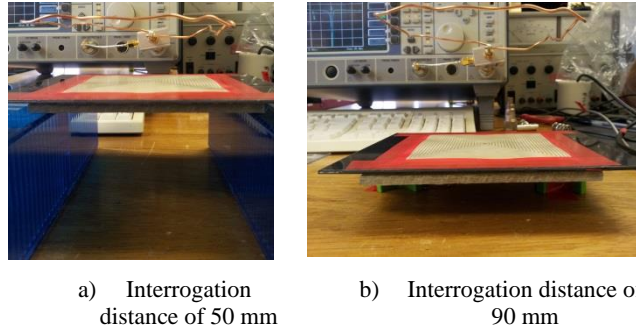
a) Interrogation distance of 50 mm

b) Interrogation distance of 90 mm

Figure 11 Wireless setup for two different interrogation distances: a) 50 mm, b) 90 mm.

The resonant frequency of the undamaged and the damaged composite, and using as reference the sensor on free-space were analysed and compared. The graph in Figure 11 shows that the sensor resonant frequencies decrease when the sample is placed close to the sensor. The fiber glass, acting as a dielectric, causing an increase in the capacitance of the system, accordingly to the formula $f = \frac{1}{2\pi\sqrt{LC}}$

(**1**, and the resonance frequency decreases. Furthermore, the presence of damage, as shown for the graph and the chart in Figure 11 cause a further decrease in the resonant frequency.
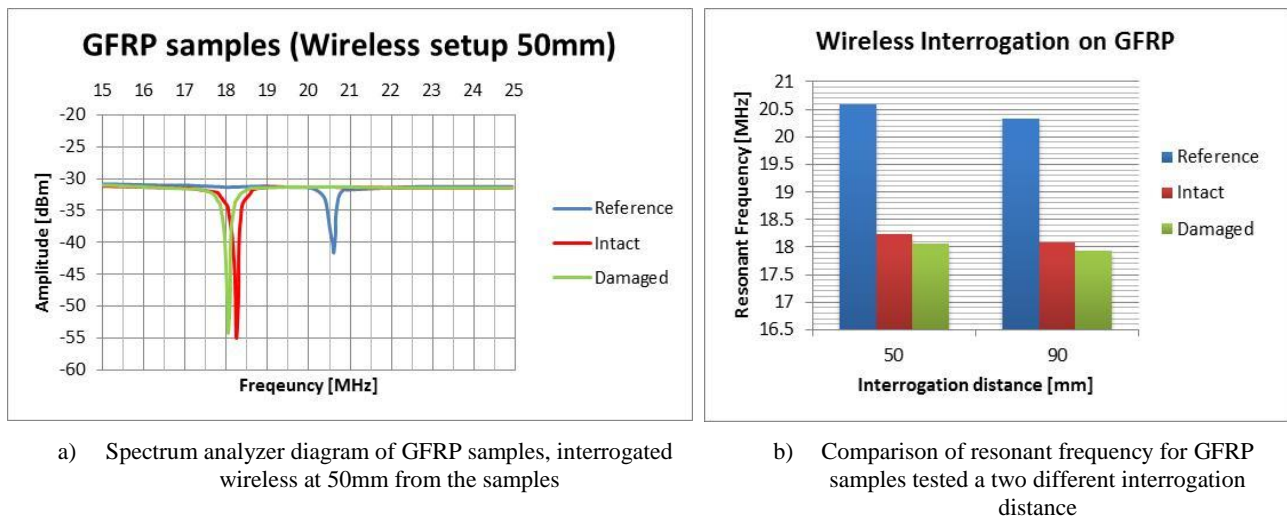

a) Spectrum analyzer diagram of GFRP samples, interrogated wireless at 50mm from the samples

b) Comparison of resonant frequency for GFRP samples tested a two different interrogation distance

Figure 12 Wireless interrogation of GFRP samples: a) Spectrum analyzer diagram; b) Comparison of different interrogation distance

3.4. Wired setup:

The wired setups allow the possibility to test conductive and non-conductive samples. Eliminating the factors related to the coupling with the antenna, more tests were performed with the wired system. Indeed, both sensors were tested, and a further detection method (Figure 13) was investigated, by connecting the sensors to the spectrum analyser using a coupler, or connecting the sensor and a loop antenna directly to the spectrum analyser and using. The latter configuration was tested using the sensor as a receiver and the antenna as interrogating device or viceversa.
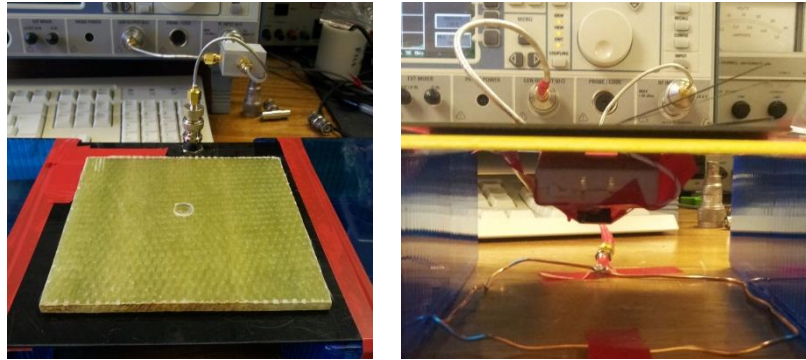
a) Sensor attached on polyimide panel wired through coupler

b) Sensor wired to the spectrum analyser to work as a receiver antenna, and interrogated by a loop antenna

Figure 13 Wired setup: a) using a coupler; b) using an external loop antenna

The resonant frequencies of each relative configuration are reported below, Figure 14 and Figure 15, grouping the result for the two typologies of material tested (CFRP and GFRP).
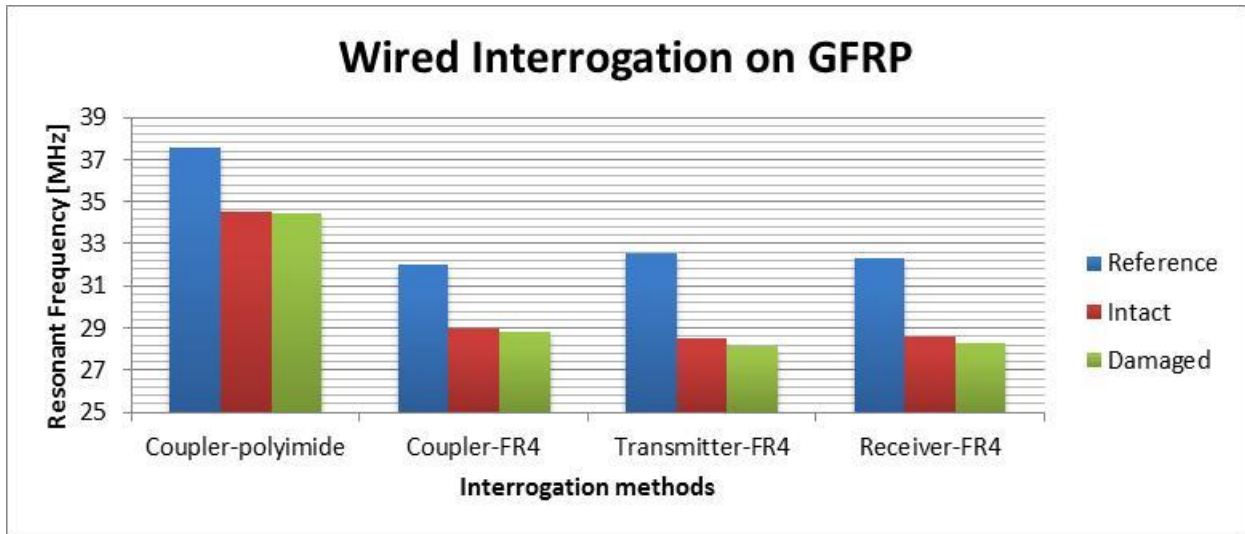

Figure 14 Comparison of Wired Interrogation methods on GFRP samples

As for the wireless system, the resonant frequency present the same trend, decreasing with the sample placed close the sensor, and with a further decrease caused by the presence of a damage. Instead the carbon composites, due their different properties, the presence of damage causes an increase of the resonant frequency (Figure 15). The sensor shows a good sensitivity also in presence of delamination.
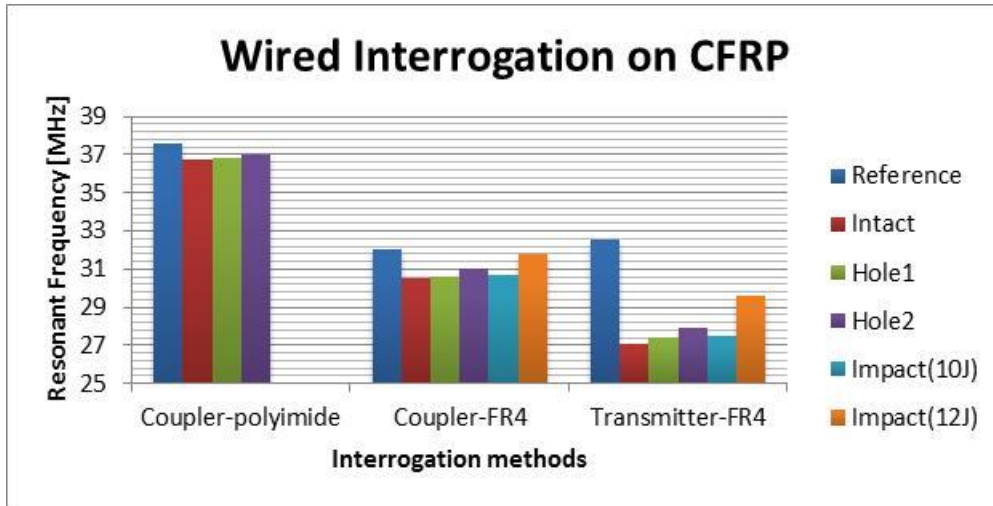
Figure 15 Comparison of Wired Interrogation methods on CFRP samples

In the transmitter mode the sensitivity of the sensor to the presence of damage increases, as it is possible to observe from the difference between the two samples impacted, and the difference between the sensor in free space and the reference sample. In this work only the resonant frequency is examined, in order to detect the damage, and it has been proved that it is a parameter sensitive to the dimension of defects. As shown in Figure 16, the different defects affect also other parameters, like the bandwidth and the amplitude of the signal. Indeed, as showed in the Figure 16a, the samples impacted present almost the same resonant frequency with respect to the reference, but present different value of amplitude and bandwidth. This leads to plan further tests, in order to obtain a more accurate diagnosis of the sample correlating the change of the mentioned parameters to the characteristic of the damage.
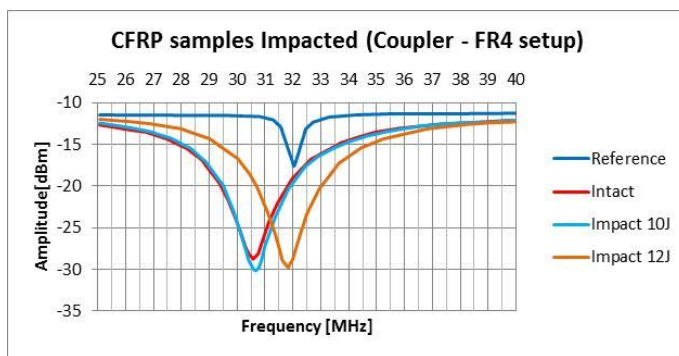
a) sensor wired with a coupler
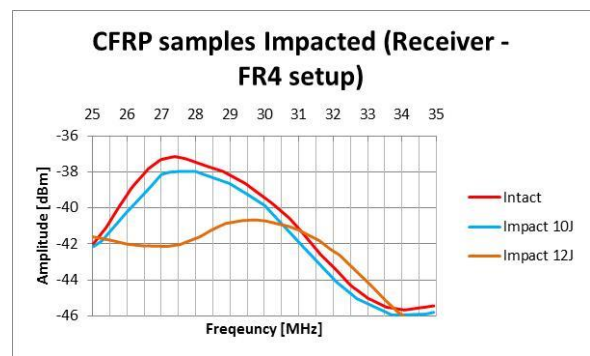
b) sensor wired, working as receiver and interrogated by a loop antenna.

Figure 16 Spectrum analyzer diagram of CFRP samples: a) sensor wired with a coupler; b) sensor wired, working as receiver and interrogated by a loop antenna.

The functionality of the sensor wireless is strictly related to the magnetic field strength and so is proportional to the interrogation distance. In order to optimize the sensitivity of the sensor and to increment the interrogation distance, more tests will be performed, based on different methods used to interrogate resonant circuits available [13, 15, 17, 23] .

4. Conclusion

A resonant sensors were developed and tested on both conductive and non-conductive materials. Compared to an undamaged sample, a shift in the resonant frequencies occurred when the sensors were placed on a damaged composite panel, thus revealing the structural defect. Moreover, an understanding of the parameters affecting the resonant frequency referred to the different types of material tested was investigated. The great advantage of the sensing system presented in this work is the ability to work either wireless interrogated by a loop antenna or wired connected to a device able to detect his resonant frequency. Indeed, as both methods work on the same principles, the former is more suitable for ground inspection, whilst the second one could be used as SHM sensor for in-situ measurements. Further manufacturing process for the sensors, using printing technique and different conductive materials (silver, CNTs) is under investigation. Furthermore, in order to optimize the sensitivity of the sensor and to increment the interrogation distance, more tests will be carried out to quantify the effect of each single parameter to the different defects, thus allowing the assessment of the severity and depth of the damage.

5. Acknowledgement

REFERENCES

[1] D. Balageas, *Structural health monitoring*, Wiley Online Library (2006).

[2] C. Farrar, "Historical overview of structural health monitoring," Lecture notes on structural health monitoring using statistical pattern recognition (2001)

[3] M. Celebi, "Seismic instrumentation of buildings (with emphasis on federal buildings)," Special GSA/USGS Project, an administrative report (2002)

[4] W. Staszewski, C. Boller and G. R. Tomlinson, *Health monitoring of aerospace structures: smart sensor technologies and signal processing*, Wiley. com (2004).

[5] M. Lin, X. Qing, A. Kumar and S. J. Beard, "SMART layer and SMART suitcase for structural health monitoring applications," in *SPIE's 8th Annual International Symposium on Smart Structures and Materials*, pp. 98-106, International Society for Optics and Photonics (2001).

[6] F.-K. Chang, *Structural Health Monitoring: The Demands and Challenges: Proceedings of the 3rd International Workshop on Structural Health Monitoring: the Demands and Challenges, Stanford University, Stanford, CA, September 12-14, 2001*, CRC Press (1999).

[7] S. W. Doebling, C. R. Farrar and M. B. Prime, "A summary review of vibration-based damage identification methods," Shock and vibration digest 30(2), 91-105 (1998)

[8] G. Bartelds, "Aircraft structural health monitoring, prospects for smart solutions from a European viewpoint," Structural Health Monitoring, Current Status and Perspectives 293-300 (1997)

[9] A. Deivasigamani, A. Daliri, C. H. Wang and S. John, "A Review of Passive Wireless Sensors for Structural Health Monitoring," Modern Applied Science 7(2), p57 (2013)

[10] J. P. Lynch, "A Summary Review of Wireless Sensors and Sensor Networks for Structural Health Monitoring," The Shock and Vibration Digest 38(2), 91-128 (2006)

[11] C. Wang, K. L. Dudley and G. N. Szatkowski, "Open Circuit Resonant (SansEC) Sensor for Composite Damage Detection and Diagnosis in Aircraft Lightning Environments," in *4th AIAA Atmospheric and Space Environments Conference* (2012).

[12] J. J. Mielnik Jr, "Open Circuit Resonant Sensors for Composite Damage Detection and Diagnosis," (2011)

[13] S. E. Woodard, B. D. Taylor, Q. A. Shams and R. G. Bryant, "Magnetic field response measurement acquisition system," Google Patents (2006).

[14] S. E. Woodard, "SansEC sensing technology—A new tool for designing space systems and components," in *Aerospace Conference, 2011 IEEE*, pp. 1-11, IEEE (2011).

[15] S. E. Woodard and B. D. Taylor, "Measurement of multiple unrelated physical quantities using a single magnetic field response sensor," Measurement Science and Technology 18(5), 1603-1613 (2007)

[16] K. J. Loh, J. P. Lynch and N. A. Kotov, "Passive wireless sensing using SWNT-based multifunctional thin film patches," International Journal of Applied Electromagnetics and Mechanics 28(1), 87-94 (2008)

[17] K. G. Ong, C. A. Grimes, C. L. Robbins and R. S. Singh, "Design and application of a wireless, passive, resonant-circuit environmental monitoring sensor," Sensors and Actuators A: Physical 93(1), 33-43 (2001)

[18] C. Neagu, H. Jansen, A. Smith, J. Gardeniers and M. Elwenspoek, "Characterization of a planar microcoil for implantable microsystems," Sensors and Actuators A: Physical 62(1), 599-611 (1997)

[19] G. Klysz, J.-P. Balayssac, X. Dérobert and C. Aubagnac, "Evaluation of cover concrete by coupling some non-destructive techniques—Contribution of in-situ measurements," in *NDT-CE conf., Berlin* (2003).

[20] A. A. Nassr and W. W. El-Dakhakhni, "Non-destructive evaluation of laminated composite plates using dielectrometry sensors," Smart Materials and Structures 18(5), 055014 (2009)

[21] U.-M. Jow and M. Ghovanloo, "Design and optimization of printed spiral coils for efficient transcutaneous inductive power transmission," Biomedical Circuits and Systems, IEEE Transactions on 1(3), 193-202 (2007)

[22] S. Roleson, "Benchtop EMC testing techniques for medical equipment," Computer Standards & Interfaces 20(6), 483 (1999)

[23] M. G. Allen and J. M. English, "System and method for the wireless sensing of physical properties," Google Patents (2000).